Characterization and application of electrochemical deposition Cdse thin films

D. N. Alhilfi[a,*], A. S. Al-Kabbib[b]
[a]*Polymer Research Center, University of Basrah, Basrah 61004, Iraq*
[b]*Department of Physics, College of Science, University of Basrah, Basrah 61004, Iraq*

The electrochemical deposition method created a CdSe thin film on FTO glass substrates. The film was examined using field scanning electron microscopy, energy dispersive spectroscopy, X-ray diffraction, Raman spectroscopy, and optical and electrochemical measurements. The results show that the CdSe nanoparticles were evenly distributed on the substrate, with a Cd/Se ratio of 63.30% Se and 36.70% Cd. The XRD revealed a polycrystalline, hexagonal structure. The film is n-type semiconductor concentration with a carrier concentration of 1.194×10^{20} cm^{-3}. The CdSe showed 552.5 mF/cm^2 of specific capacity with energy and a power density of 2.5 mW/cm^2 and 9000 mW/cm^2, respectively.

(Received June 5, 2024; August 13, 2024)

Keywords: CdSe, Electrodeposition, Electrochemical impedance, Supercapacitors

1. Introduction

Many researchers are interested in thin films of II-VI compound semiconductors because they have applications in solid-state physics. CdSe is comprising cadmium (Cd) and selenium (Se). It is a semiconducting material that exhibits unique optical and electrical properties. CdSe is widely used in various applications, particularly in optoelectronics and nanotechnology. Cadmium selenide (CdSe) is a popular semiconductor material in the II-VI group due to its suitable band gap (1.74 eV).[7] In addition to its optoelectronic applications, CdSe is also used in nanotechnology. CdSe nanoparticles can be functionalized and incorporated into various materials, including polymers and composites, to impart specific properties or functions[8]. In biological imaging, they can be used as fluorescent probes [9] or electronic device components. Cadmium selenide exists in two polymorph modifications: cubic and hexagonal[10]. Cubic (sphalerite-type structure), while hexagonal (wurtzite-type structure). At 350–400 °C, cubic cadmium selenide is converted to hexagonal cadmium selenide[11].

CdSe thin films have been deposited using a variety of deposition techniques, including vacuum evaporation[12], liquid phase deposition[13], molecular beam epitaxy [14], closed space sublimation [15] chemical bath deposition [16], and Electrodeposition [10]. One of the methods to synthesize CdSe nanoparticles is electrodeposition. This technique involves applying an electric potential to a substrate immersed in an electrolytic solution containing cadmium and selenium ions. Electrodeposition can produce CdSe nanoparticles and thin films with various morphologies, structures, and compositions depending on the deposition parameters, such as potential, current, pH, temperature, and substrate type[17]. Electrodeposition is one of the simplest and least expensive methods since it is easy to set up and maintain.

This study aims to provide detailed information on the crystalline and morphological structure and the optical characterization of CdSe thin film produced by the electrodeposition method using cadmium acetate as the source for cadmium. Electrochemical measurements constitute an effective tool to probe the quality of prepared thin films. So, this study offers a comprehensive discussion of the results of electrochemical measurements on nanocrystalline CdSe thin film.

* Corresponding authors: dalal.munshid@uobasrah.edu.iq
https://doi.org/10.15251/CL.2024.218.641

2. The experimental

Two electrodes were prepared at room temperature at 3-volt for 30 minutes, and the CdSe thin films were deposited. Platinum was the counter electrode, while fluorine-doped Tin Oxide (FTO) glass (surface resistivity 8–15Ω) was the working electrode. The pH value of an aqueous electrolyte consisting of 0.1M cadmium acetate [Cd $(CH3COO)_2$] and 0.1 mM SeO_2 (Sigma, 98%) was adjusted by using HCL dilute. Before deposition, the substrate is cleaned with ethanol and diluted HCL 10%, acetone, and deionized water (DIW). It is then washed ultrasonically and dried with a nitrogen dryer.

Field Scanning electron microscopy (MIRA3-TESCAN) examined the film's surface morphology. Philips PW 3710 X'pert diffractometer with filtered CuKα radiation (λ = 1.54178 Å) has been used in the XRD measurements from 10° to 90°. The Raman spectra for CdSe thin film were recorded using a portable Raman spectrometer JD-532S with argon-ion laser at 532 nm excitation wavelength at room temperature. A computer-controlled spectro-photometer (Shimazdu 1800) was also used to UV-Vis thin film absorbance spectra. The thin film's photoluminescence spectrum was recorded using a luminescence spectrophotometer. The Schottky diode diagnosed electrical properties using a Keithley 2400 programmable current source. Cyclic voltammetry, Mott Schottky, and EIS were used to characterize the electrochemical behaviour of thin film using a CorrTest Workstation (CorrTest, China).

3. Result and discussion

3.1. CdSe thin film characterization

An FESEM image of as-deposited CdSe thin films at 10,000 magnifications is shown in Fig.1. A uniform distribution of spherical crystallite agglomerates has been observed on the surface of the CdSe film. It is scattered over the FTO substrate without cracks or aggregates. From the FSEM micrograph, the nanoparticle size distribution for CdSe has been found and presented in Fig .1, where the average particle size is 25–30 nm.

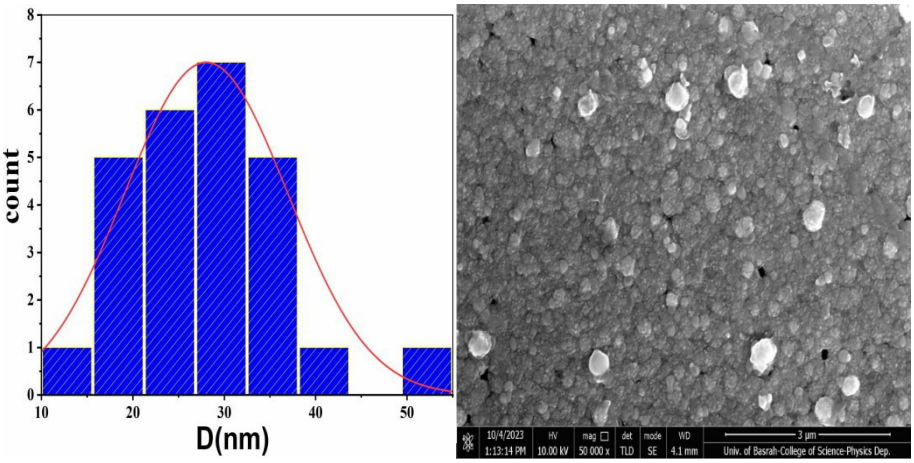

Fig. 1. The FSEM images of CdSe are thin films.

From the EDS measurement in fig. 2, the Se-rich CdSe thin films have been found where the elemental composition equals 63.30% of Se and 36.70% of Cd. Ritika C. et al. got the same results and attributed this to the high reactivity of Se ions as compared to Cd ions[18]

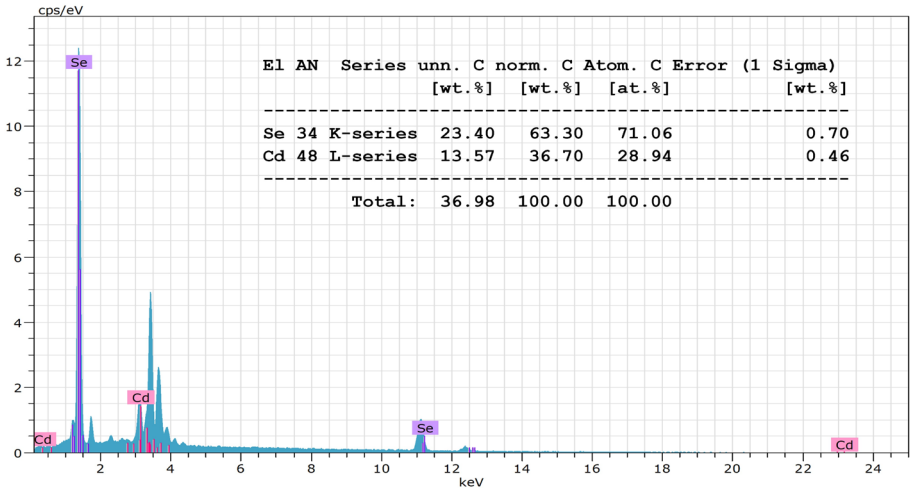

Fig. 2. The E.D.S. spectrum of CdSe thin film.

The XRD result of the CdSe thin film is shown in Fig. 3. Five sharp peaks are observed at 2θ =25.302º, 29.89º, 35.01º, 59.9 º and 72.09 º, matching the hkl planes (002), (101), (102), (201) and (212), respectively. According to (JCPDS 08 - 0459), CdSe thin films prepared by electrodeposition have a hexagonal wurtzite structure, and no peaks associated with impurities were observed. That is in agreement with previous studies preparing CdSe thin films.[19]. Although cadmium acetate is not typically used in the electrochemical method of preparing semiconductors, this proves it can be done. Debye Scherrer's Eq.1 has been used to find the crystalline size of the thin film:[20]

$$D = \frac{0.9\lambda}{\beta \cos\theta} \quad (1)$$

The wavelength (λ) of the CuKα line, the diffraction angle(θ), and β are full width at half maximum.

The inset of Fig. 3 shows the favorite diffraction peak's profile blow-up. (002); the crystallite size calculated from this peak is 19.11nm.

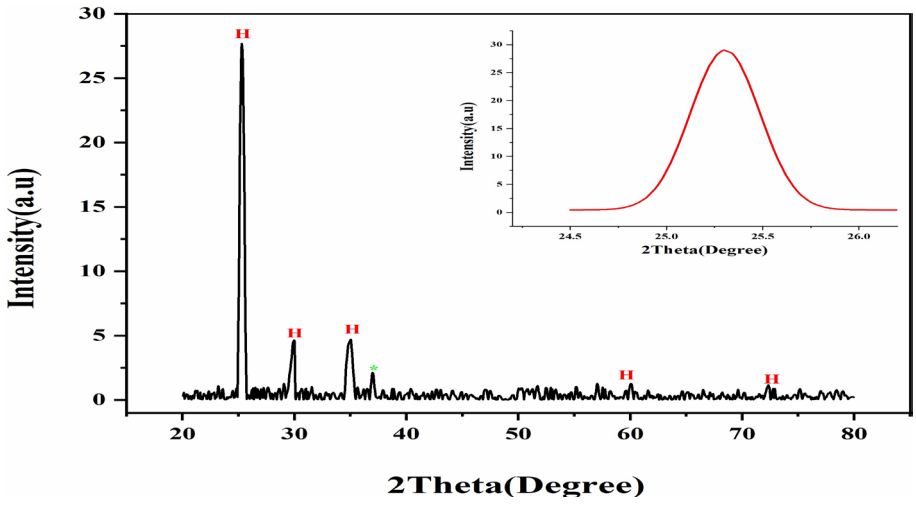

Fig. 3. The XRD of CdSe thin film prepared by electrodeposition.

The thin film in this study shows a Raman peak at 210 cm^{-1} and 420 cm^{-1}, respectively; Fig.4. The first and second LOs were identified [21]. The formation of the CdSe thin film is confirmed by the observed LO phonon frequency near the standard bulk LO frequency. The Raman shift in (LO) phonon frequency is mainly caused by the strain that developed during deposition and the nanocrystalline thin film.

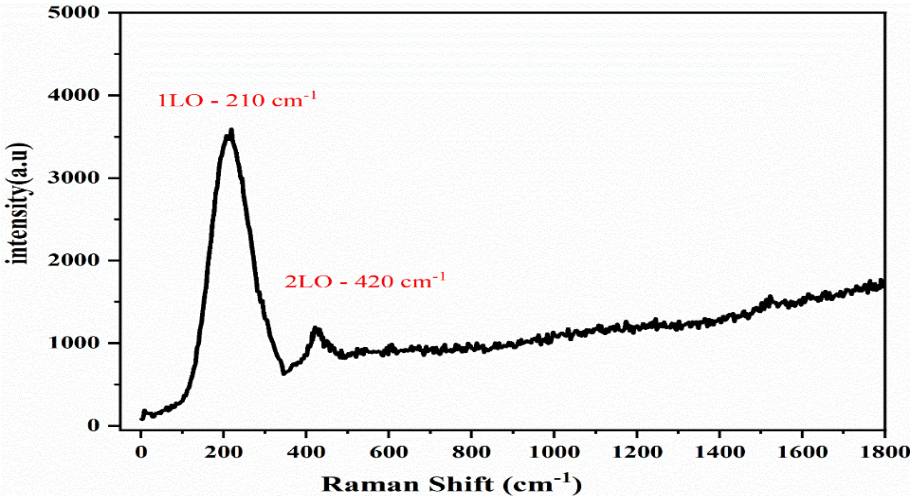

Fig. 4. Raman Spectra of CdSe thin films prepared by electrodeposition.

3.2. Optical properties

An optical absorbance measurement was conducted at room temperature to determine the optical absorbance of CdS thin films. As shown in Fig.5, An absorption peak near the visible spectrum's edge is visible in the CdSe thin film's absorption spectra. A near-infrared constant value was attained after a steady decline with increasing wavelengths. The prepared CdSe films have excellent visible-light absorption characteristics, making them for solar cells. The absorbance characteristics of CdSe are affected by many physical variables, such as the structure, morphology, and density of defects.[22], [23]. By Tauc equation 2, we determined the energy gap of the CdSe.

$$\alpha = \frac{A(h\nu - E_g)^n}{h\nu} \quad (2)$$

Where α, E_g, hν, A are the absorption coefficient, the optical band gap, the photon energy, and constants, respectively.[24]

The energy gaps of the CdSe films were predestined based on the $(\alpha h\nu)^2$ versus photon energy (hν), Fig.5CdSe films prepared by electrodeposition contain linear segments in the high energy region, confirming that they have a direct band gap and their intercept on the hν axis gives the optical band gap equal to 2.12 eV. There is good agreement between these band gap values and earlier studies[25].With decreasing particle size, the absorption edge shifts blue. As a result of quantum confinement, the absorbance curve shifts blue.[26, 27].

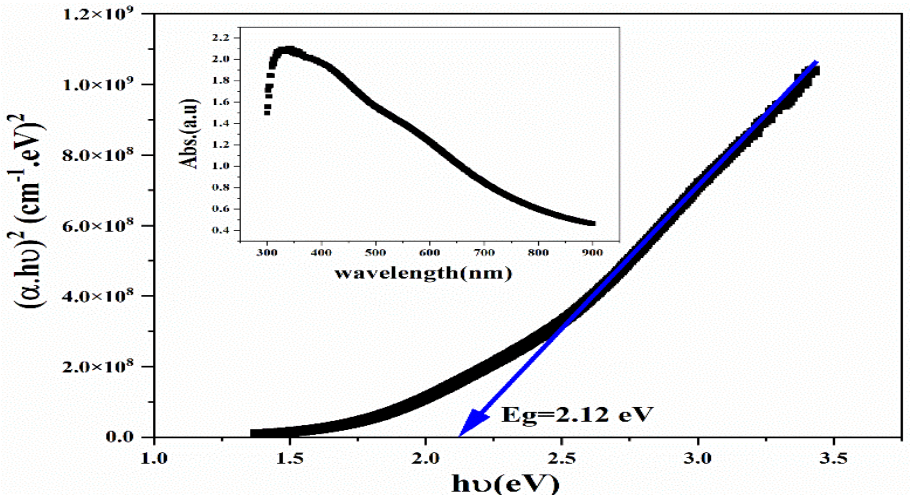

Fig. 5. The change of $(\alpha h\nu)^2$ against hν for the direct band gap of CdSe; moreover, the inset displays the absorption spectrum.

3.3. Mott–Schottky (MS)

By measuring capacitance against applied potential, it is possible to identify more parameters such as flat band potential (V_{Fb}), donor density (N_D) and the electrode's conductivity type. A semiconductor's donor density and flat band potential can be calculated using the Mott-Schottky equation[28]

$$\frac{1}{C^2} = \left(\frac{2}{e\varepsilon_0\varepsilon_r N_D}\right)\left(V - V_{Fb} - \frac{K.T.}{e}\right) \quad (3)$$

Where C, V, e, ε_r, ε_o, K and T are the space-charge capacitance, the applied voltage is the electronic charge relative to the permittivity of the deposited film (~ 10 for CdSe), the permittivity of free space (8.85 × 10–14 F cm−1), K is Boltzmann constant and T is Kelvin temperature [29]. The Mott–Schottky (M-S) curves are shown in Fig. 6, obtained under dark conditions at 300 kHz in a 1 M Na_2SO_3 electrolyte. M-S curves with positive slopes indicate n-type thin film, and the carrier density $N_{.D.}$ can be estimated from the following.

$$N_D = \frac{2}{Slope \times e\varepsilon_o\varepsilon_r} \quad (4)$$

The density of donors is determined to be $1.194 \times 10^{20} cm^{-3}$. By electrodeposition, the Mott-Schottky approximation method has been used by Russak et al., and they found that the donor density is ~ $10^{17} cm^{-3}$ and ~ 10^{20} cm^{-3} for n-type CdSe material and thin films, respectively[30]. An increase in the donor density of CdSe electrodes results in more charge carriers, which facilitates electrical conduction and may account for the improved performance of PECs.

An extrapolation of the linear portion of the M-S curve to $C^{-2} = 0$ will yield the flat band potential. The flat band potential of a semiconductor thin film can be used to determine its Fermi level, conduction band edge, and valence band edge. The Fermi level of the semiconductor (E_f) equals V_{Fb}, which equals -1.046 (V per S.C.E.) for the CdSe thin film. From relationship (5), the energy between the E_c (conduction band edge) and E_f can be determined [31]

$$\left(E_C - E_f\right) = -K.T.ln\left[\frac{N_D}{N_C}\right] \quad (5)$$

Where the density of states (N_C) in the conduction band of a semiconductor is found by [29]

$$Nc = 2\left\{\left(\frac{2\pi m_e^* K.T.}{h^2}\right)\right\}^{3/2} \quad (6)$$

The Plank constant (h) and me*= $0.12m_o$, the effective mass, where m_o equals 9.1×10^{-31} Kg for CdSe. The E_V value is calculated using the $E_C = E_V + Eg$ relation, where the E_g value is found from the UV–vis data. The results are listed in Table (1).

Table 1. All parameters were obtained from the Mott-Schottky plot of CdSe.

Physical parameters ↓→	**values**
V_{Fb} (V per SCE)	-1.046
N_D (cm^{-3})	1.194×10^{20}
N_C (cm^{-3})	1.043×10^{18}
E_c-E_f (eV per SCE)	0.123
Conduction band edge, E_C (eV per SCE)	-1.169
Band gap energy, E_g (eV)	2.057
Valence band edge, E_v (eV per SCE)	0.88
carriers' type	n-type

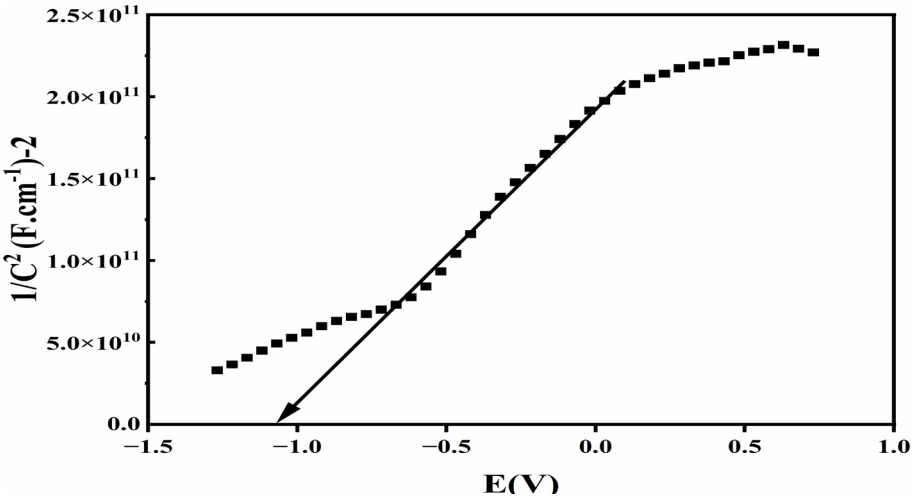

Fig. 6. Mott–Schottky (MS) curves for CdSe.

3.4. Electrochemical impedance spectroscopy studies (EIS)

The frequency range of EIS measurement is 100 kHz to 15 mHz, as demonstrated in fig.7. Nyquist plots of the thin film are employed to fit an analogous electronic circuit, allowing for finding the circuit elements' values. Z view' software fitting electronic circuit in Fig. 7 contains the solution (R_s)and charge transfer resistance between the CdSe coating and the aqueous Na_2SO_4 electrolyte (Rin) and the charge transfer resistance between the electrolyte/counter electrode (R_{out}), CPE_{in} and CPE_{out} are constant phase elements of the capacitance corresponding to R_s, R_{in} a, R_{out}. , CPE_{in} and CPE_{out} are 33.92, 0.99, 3.522, 53816 and 0.9, respectively. The chi-squared value ($\chi2$) is the goodness of the fitting data of EIS, which is accepted when $\chi^2 \approx 2.14\times10^{-4}$. The low values of R_{in} and CPE_{in} were found to be favorable for electron transport. An increased charge transfer resistance with higher capacitance leads to a decreased electron transfer rate.

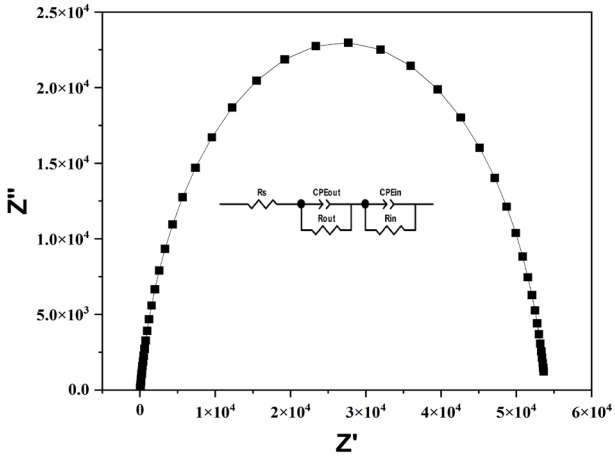

Fig. 7. The Nyquist scripts for CdSe films. An electronic circuit is displayed in the inset.

3.5. Charge-discharge measurement (GCD)

Fig.8 shows charge-discharge curves (GCD) of the CdSe electrode at 100 µA/cm current densities. The specific capacitance (C_s), the energy density (E_d) and the power density (P_d) can be calculated from the discharge time (t_D) by using Equations[32].

$$C_s = \frac{I\Delta t}{s\Delta V} \tag{7}$$

$$E = \left(\frac{C_p \Delta v^2}{2}\right)\Big/_{3.6} \tag{8}$$

$$P = \frac{3600 \times E}{\Delta t} \tag{9}$$

Where ΔV is the potential window, Δt is the discharge time, and s is the thin film surface area. The C_p, P and E values are found to be equal to 552.5 mF/cm^2, 2.5 mWh/cm^2 and 9000 mW/ cm^2, respectively. The reduced Rct exhibited a significant increase in the conductivity of the CdSe electrode, leading to improved energy storage capabilities.

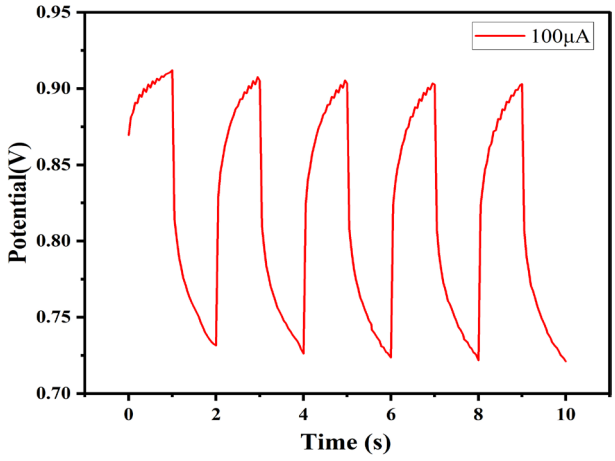

Fig. 8. Charge discharge measurements of CdSe thin film.

4. Conclusions

This work describes the results of detailed experimental evaluations on CdSe thin films created by electrodeposition of CdSe thin films. The films have a polycrystalline structure and an average crystallite size of 23.87 nm. The thin film displays a homogeneous surface consisting of almost spherical nanoparticles. The predicted energy band gap (Eg) is 2.12 eV according to optical absorbance. The Mott-Schottky results demonstrated that the CdSe thin films are n-type, and the carrier concentration (n) is determined to be equal to 1.194×10^{20} cm^{-3}. Based on the EIS Analysis, the low values of Rct and capacitance were found to ensure minimal diffusion obstruction when the electrons are transported in the CdSe/electrolyte interface. Charge-discharge measurement shows C_p equals 552.5 mF/cm^2 with energy and power density 2.5 mWh/cm^2 and 9000 mW/cm^2, respectively. These results indicate the possibility of using the prepared CdSe thin films in various electronic device applications.

References

[1] K. Nemoto, J. Watanabe, H. Yamada, H.-T. Sun, N. Shirahata, Nanoscale Adv., 2023; https://doi.org/10.1039/D2NA00734G

[2] M. Davoodi, F. Davar, S. Mandani, B. Rezaei, A. E. Shalan, Ind. Eng. Chem. Res., vol. 62, no. 6, pp. 3050-3052, 2023; https://doi.org/10.1021/acs.iecr.2c01776

[3] Y. Araki, K. Ohkuno, T. Furukawa, J. Saraie, J. Cryst. Growth, vol. 301-302, no. SPEC. ISS., pp. 809-811, 2007; https://doi.org/10.1016/j.jcrysgro.2006.11.105

[4] D. Yao, Z. Hu, L. Zheng, S. Chen, W. Lü, H. Xu, Appl. Surf. Sci., vol. 608, p. 155230, 2023; https://doi.org/10.1016/j.apsusc.2022.155230

[5] G. Sreedhar, A. Sivanantham, S. Venkateshwaran, S. K. Panda, M. Eashwar, J. Mater. Chem. A, vol. 3, no. 25, pp. 13476-13482, 2015; https://doi.org/10.1039/C5TA00304K

[6] J. Liu, Dong Liu, S. Liu, Jie Liu, H. Wang, Chenglei Ge, Zhongwei Hao, Xiaotao Du, Na Xiao, Phys. E Low-Dimensional Syst. Nanostructures, vol. 115, no. July 2019, 2020; https://doi.org/10.1016/j.physe.2019.113669

[7] R. Chowdhury et al., Dhaka Univ. J. Sci., vol. 60, no. 1, pp. 137-140, Apr. 2012; https://doi.org/10.3329/dujs.v60i1.10352

[8] S. Li, M. Meng Lin, M. S. Toprak, D. K. Kim, M. Muhammed, Nano Rev., vol. 1, no. 1, p. 5214, 2010; https://doi.org/10.3402/nano.v1i0.5214

[9] H. D. Duong, J. Il Rhee, Sensors (Switzerland), vol. 19, no. 22, 2019; https://doi.org/10.3390/s19224977

[10] S. M. Rashwan, S. M. Abd El-Wahab, M. M. Mohamed, J. Mater. Sci. Mater. Electron., vol. 18, no. 6, pp. 575-585, Jun. 2007; https://doi.org/10.1007/s10854-007-9141-8

[11] O. Portillo-Moreno, R. Lozada-Morales, M. Rubın-Falfán, J. A. Perez-Alvarez, O. Zelaya-Angel, L. Banos-Lopez, J. Phys. Chem. Solids, vol. 61, no. 11, pp. 1751-1754, 2000; https://doi.org/10.1016/S0022-3697(00)00051-2

[12] K. R. Murali, K. Srinivasan, D. C. Trivedi, Mater. Lett., vol. 59, no. 1, pp. 15-18, 2005; https://doi.org/10.1016/j.matlet.2004.09.006

[13] C. E. Hamilton, D. J. Flood, A. R. Barron, Phys. Chem. Chem. Phys., vol. 15, no. 11, pp. 3930-3938, 2013; https://doi.org/10.1039/c3cp50435b

[14] R. Livingstone, X. Zhou, M. C. Tamargo, J. R. Lombardi, L. G. Quagliano, F. Jean-Mary, J. Phys. Chem. C, vol. 114, no. 41, pp. 17460-17464, Oct. 2010; https://doi.org/10.1021/jp105619m

[15] V. T. Patil, Y. R. Toda, V. P. Joshi, D. A. Tayade, J. V. Dhanvij, D. N. Gujarathi, Chalcogenide Lett., vol. 10, no. 7, pp. 239-247, 2013.

[16] K. Sarmh, K. K. Borah, Trends Sci., vol. 20, no. 1, p. 3530, 2023; https://doi.org/10.48048/tis.2023.3530

[17] S. I. Ozmen H. M. Gubur, Bull. Mater. Sci., vol. 45, no. 2, p. 77, 2022; https://doi.org/10.1007/s12034-021-02653-6

[18] R. Choudhary, R. P. Chauhan, Electron. Mater. Lett., vol. 13, no. 4, pp. 330-338, Jul. 2017; https://doi.org/10.1007/s13391-017-6231-5

[19] K. Sharma, A. S. Al-Kabbi, G. S. S. Saini, S. K. Tripathi, J. Alloys Compd., vol. 651, pp. 42-48, Dec. 2015; https://doi.org/10.1016/j.jallcom.2015.08.038

[20] A. S. Al-Kabbi, K. Sharma, G. S. S. Saini, S. K. Tripathi, Phys. Scr., vol. 87, no. 2, p. 25604, 2013; https://doi.org/10.1088/0031-8949/87/02/025604

[21] M. Ichimura, K. Takeuchi, A. Nakamura, E. Arai, Thin Solid Films, vol. 384, no. 2, pp. 157-159, Mar. 2001; https://doi.org/10.1016/S0040-6090(00)01826-5

[22] S. Z. Werta, O. K. Echendu, F. B. Dejene, Z. N. Urgessa, J. R. Botha, Appl. Phys. A Mater. Sci. Process., vol. 124, no. 9, p. 0, 2018; https://doi.org/10.1007/s00339-018-1996-4

[23] A. G. Habte, F. G. Hone, F. B. B. Dejene, Inorg. Chem. Commun., vol. 103, pp. 107-112, May 2019; https://doi.org/10.1016/j.inoche.2019.03.017

[24] S. K. Tripathi, A. S. Al-Kabbi, K. Sharma, G. S. S. Saini, Thin Solid Films, vol. 548, pp. 406-410, Dec. 2013; https://doi.org/10.1016/j.tsf.2013.09.008

[25] P. P. Hankare et al., J. Phys. Chem. Solids, vol. 67, no. 12, pp. 2506-2511, 2006; https://doi.org/10.1016/j.jpcs.2006.07.006

[26] S. Chaure, N. B. Chaure, R. K. Pandey, Phys. E Low-Dimensional Syst. Nanostructures, vol. 28, no. 4, pp. 439-446, 2005; https://doi.org/10.1016/j.physe.2005.05.044

[27] R. Jain, V. K. Verma, Phosphorus, Sulfur Silicon Relat. Elem., vol. 190, no. 11, pp. 1749-1754, Nov. 2015; https://doi.org/10.1080/10426507.2015.1031754

[28] S. Zhang, R. Shi, Y. Tan, J. Alloys Compd., vol. 711, pp. 155-161, 2017; https://doi.org/10.1016/j.jallcom.2017.03.327

[29] H. Bayramoglu, A. Peksoz, Mater. Sci. Semicond. Process., vol. 90, pp. 13-19, Feb. 2019; https://doi.org/10.1016/j.mssp.2018.09.021

[30] M. A. Russak, J. Reichman, H. Witzke, S. K. Deb, S. N. Chen, J. Electrochem. Soc., vol. 127, no. 3, p. 725, 1980; https://doi.org/10.1149/1.2129740

[31] V. S. Raut, C. D. Lokhande, V. V. Killedar, J. Electroanal. Chem., vol. 788, pp. 137-143, 2017; https://doi.org/10.1016/j.jelechem.2017.02.010

[32] L. Teng, L. Tian, W. Li, H. Feng, Z. Xing, Synth. Met., vol. 291, p. 117169, 2022; https://doi.org/10.1016/j.synthmet.2022.117169

[33] V. D. Das, L. Damodare, J. Appl. Phys., vol. 81, no. 3, pp. 1522-1530, Feb. 1997; https://doi.org/10.1063/1.363913

[34] T. J. Coutts, Thin Solid Films, vol. 50, no. 1978, pp. 99-117, May 1978; https://doi.org/10.1016/0040-6090(78)90096-2

[35] A. Jana, M. Hazra, J. Datta, Journal of Solid State Electrochemistry, vol. 21, no. 11. pp. 3083-3091, 2017; https://doi.org/10.1007/s10008-017-3656-6